GSA Data Repository 2016036

Age of the Laschamp excursion determined by U-Th dating of a speleothem geomagnetic record from North America

Ioan Lascu et al.

MAGNETIC METHODS

The slab used for paleomagnetism, with a cross section of 1.7 cm × 0.7 cm, was sectioned into 38 specimens, ~0.5 cm in thickness each. After measuring the natural remanent magnetization (NRM), each specimen was demagnetized in stepwise fashion with a D-Tech 2000 alternating frequency (AF) demagnetizer, using peak fields progressively increasing on a logarithmically-spaced scale from 0.5 mT until the magnetization reached magnetometer noise levels (~10^{-11} Am^2). Remanence at each step was independently measured 30 times on each specimen using a 2G Enterprises superconducting quantum interference device magnetometer. Measurements with high noise/signal ratios were excluded from the calculation of the average values. Standard deviations were on the order of 1 nAm^2/kg. The characteristic remanence was isolated via principal component analysis (Kirschvink, 1980) using PuffinPlot (Lurcock and Wilson, 2012). We adopted the protocol devised by Peppe et al. (2009) for weak specimens, as follows: to define the characteristic remanence component we used either a) the best-fit line through a minimum of three consecutive demagnetization steps that trended toward the origin and had a maximum angular deviation (MAD) less than 20° (for specimens with quasi-linear trajectories, e.g., Figs. DR2, 2C-D), or b) a minimum of 4 consecutive demagnetization steps anchored to the origin, with MAD <20° (for specimens with directions clustering around one point, e.g., Fig. 2E). Because the speleothem is not azimuthally oriented, declination values were rotated so that average baseline values were situated in the interval [-10°, 30°], corresponding to realistic field declination values at the time in North America (e.g., Lund et al., 2005; Channell, 2006; Böhnel and Molina-Garza, 2002; Negrini et al., 2014).

Mean declination was obtained by averaging adjusted declinations in the considered azimuthal interval at 1° increments. Virtual geomagnetic pole (VGP) coordinates were calculated at each adjusted declination step, and then combined to obtain mean and standard deviation values. After completing the NRM demagnetization, anhysteretic remanent magnetization (ARM) was imparted in the presence of a 0.05 mT bias field superimposed on an AF field decaying from a peak value of 100 mT, at a rate of 5 μT per half cycle. ARM susceptibility (χ_{ARM}) was calculated by normalizing the ARM to the bias field. Isothermal remanent magnetization (IRM) was imparted in a 1 T direct field using an impulse magnetizer. The ARM/IRM ratio (χ_{ARM}/IRM), computed by normalizing the ARM susceptibility by the IRM, is used as a magnetic grain size indicator, with higher values indicating finer bulk magnetic grain size.

Additional discrete (<500 mg) specimens from the speleothem were used for low temperature magnetic measurements to determine magnetic mineralogy. Low temperature saturation IRM was imparted in a 2.5 T field at 10 K following two separate treatments: field cooling in a 2.5 T field and zero-field cooling, from 300 to 10 K. Remanence behavior was then measured in zero field at 5 K intervals upon warming to room temperature. Finally, the behavior of a room temperature saturation IRM imparted in a 2.5 T field was measured in zero field at 5 K intervals while cooling the sample down to 10 K and then warming it back to 300 K.

REFERENCES CITED

Böhnel, H., and Molina-Garza, R., 2002, Secular variation in Mexico during the last 40,000 years: Physics of the Earth and Planetary Interiors, v. 133, p. 99–109.

Channell, J., 2006, Late Brunhes polarity excursions (Mono Lake, Laschamp, Iceland Basin and Pringle Falls) recorded at ODP Site 919 (Irminger Basin): Earth and Planetary Science Letters, v. 244, no. 1-2, p. 378–393, doi: 10.1016/j.epsl.2006.01.021.

Kirschvink, J.L., 1980, The least-squares line and plane and the analysis of paleomagnetic data: Geophysical Journal of the Royal Astronomical Society, v. 62, p. 699–718.

Lund, S.P., Scwartz, M., Keigwin, L., and Johnson, T., 2005, Deep-sea sediment records of the Laschamp geomagnetic field excursion (~41,000 calendar years before present): Journal of Geophysical Research, v. 110, B04101, doi: 10.1029/2003JB002943.

Lurcock, P.C., and Wilson, G.S., 2012, PuffinPlot: A versatile, user-friendly program for paleomagnetic analysis: Geochemistry, Geophysics, Geosystems, v. 13, no. 6, Q06Z45, doi: 10.1029/2012GC004098.

Negrini, R.M., McCuan, D.T., Horton, R.A., Lopez, J.D., Cassata, W.S., Channell, J.E.T., Verosub, K.L., Knott, J.R., Coe, R.S., Liddicoat, J.C., Lund, S.P., Benson, L. V, and Sarna-Wojcicki, A.M., 2014, Nongeocentric axial dipole field behavior during the Mono Lake excursion: Journal of Geophysical Research, v. 119, p. 2567–2581, doi: 10.1002/2013JB010846.

Peppe, D.J., Evans, D.A.D., and Smirnov, A.V., 2006, Magnetostratigraphy of the Ludlow Member of the Fort Union Formation (Lower Paleocene) in the Williston Basin, North Dakota: Geological Society of America Bulletin, v. preprint, no. 2008, p. 1, doi: 10.1130/B26353.1.

Table DR1. ^{230}Th dating results. The error is 2σ

Sample depth (mm)	^{238}U (ppb)		^{232}Th (ppt)		^{230}Th / ^{232}Th (atomic x10^{-6})		δ^{234}U* (measured)		^{230}Th / ^{238}U (activity)		^{230}Th Age (yr) (uncorrected)		^{230}Th Age (yr) (corrected)		δ^{234}U$_{Initial}$† (corrected)		^{230}Th Age (yr BP)§ (corrected)	
1.90 ±0.30	790	±1	18977	±380	612	±12	3507.5	±3.3	0.8925	±0.0015	23399	±48	23252	±115	3745	±4	23189	±115
13.45 ±0.25	688	±1	4537	±91	2921	±59	3079.8	±3.5	1.1679	±0.0022	35237	±82	35193	±87	3401	±4	35130	±87
23.00 ±0.50	778	±1	941	±19	16874	±342	2935.3	±4.3	1.2375	±0.0030	39250	±121	39242	±121	3279	±5	39179	±121
30.95 ±0.35	1003	±2	835	±17	24854	±504	2835.8	±3.9	1.2548	±0.0032	41102	±132	41096	±132	3184	±5	41033	±132
37.80 ±0.30	828	±1	489	±10	35313	±722	2780.2	±3.3	1.2656	±0.0024	42234	±101	42230	±101	3132	±4	42167	±101
49.40 ±0.30	772	±1	520	±11	31206	±639	2641.8	±2.8	1.2757	±0.0024	44560	±106	44556	±106	2996	±3	44493	±106
82.10 ±0.40	580	±1	1512	±30	8627	±174	2451.1	±2.8	1.3647	±0.0022	51538	±114	51518	±114	2835	±3	51455	±114
116.45 ±0.35	648	±1	5408	±108	2863	±58	2441.3	±3.5	1.4493	±0.0032	55650	±167	55587	±173	2856	±4	55524	±173
150.90 ±0.50	550	±1	36857	±739	365	±7	2308.2	±3.3	1.4856	±0.0032	60317	±181	59793	±412	2732	±5	59730	±412
185.80 ±0.80	449	±1	10149	±203	1157	±23	2335.8	±2.9	1.5854	±0.0031	64768	±177	64595	±215	2803	±4	64532	±215

U decay constants: λ_{238} = 1.55125x10^{-10} (Jaffey et al., 1971) and λ_{234} = 2.82206x10^{-6} (Cheng et al., 2013). Th decay constant: λ_{230} = 9.1705x10^{-6} (Cheng et al., 2013).

*$\delta^{234}U = ([^{234}U/^{238}U]_{activity} - 1)x1000$.

†$\delta^{234}U_{initial}$ was calculated based on ^{230}Th age (T), i.e., $\delta^{234}U_{initial} = \delta^{234}U_{measured} \times e^{\lambda_{234} \times T}$.

Corrected ^{230}Th ages assume the initial ^{230}Th/^{232}Th atomic ratio of 4.4 ±2.2 x10^{-6}. Those are the values for a material at secular equilibrium, with the bulk earth ^{232}Th/^{238}U value of 3.8. The errors are arbitrarily assumed to be 50%.

§B.P. stands for “Before Present” where the “Present” is defined as the year 1950 A.D.

Table DR2. Paleomagnetic and rock magnetic time series

Age (yr BP)	NRM (Am2/kg)	ARM (Am2/kg)	IRM (Am2/kg)	NRM/ARM	χ_{ARM}/IRM (mm/A)	Declination (degrees)	Inclination (degrees)	VGP Latitude (degrees)	VGP Latitude error (degrees)
23292	5.33E-07	2.56E-06	6.25E-05	0.207922	0.515064	28.26	52.67	66.6	10.7
27944.6	4.75E-08	8.34E-08	1.29E-06	0.569124	0.81343	19.49	49.38	71.3	9.3
33114.1	1.42E-07	2.70E-07	6.42E-06	0.524644	0.529256	30.46	53.68	65.2	10.7
36423.2	8.23E-08	1.69E-07	2.82E-06	0.487076	0.75422	-15.56	46.81	72	7.9
38542.9	8.45E-08	9.81E-08	2.35E-06	0.862019	0.524338	34.17	65.11	63.2	9.1
39995	1.13E-08	3.68E-08	5.01E-07	0.306445	0.922701	84.89	30.47	14	10.6
41103.1	3.73E-09	4.71E-08	4.73E-07	0.0791692	1.25149	133.79	11.32	-28.3	8.8
41910.1	5.23E-09	2.96E-08	4.21E-07	0.176279	0.884015	28.23	9.82	47.3	7.4
42858.4	2.79E-08	4.47E-08	5.58E-07	0.62411	1.00707	12.99	56.03	78	8.8
43845.9	1.66E-08	3.85E-08	5.42E-07	0.430773	0.892482	-4.87	57.31	80.8	6.2
44843.8	2.33E-08	4.75E-08	8.09E-07	0.490018	0.737676	67.55	66.02	41.3	8.8
45897.7	5.00E-08	6.30E-08	9.53E-07	0.793532	0.831496	10.50	75.71	62.9	2.1
46941	3.51E-08	6.10E-08	1.64E-06	0.576282	0.465807	33.40	29.22	52.5	9.2
47973.6	4.29E-08	5.99E-08	1.10E-06	0.715997	0.682593	4.97	53.26	79.3	5.5
49016.9	3.09E-08	6.95E-08	1.09E-06	0.444806	0.802337	4.76	43.75	73.6	4
50070.8	3.19E-08	5.24E-08	8.62E-07	0.608729	0.763337	19.49	46.98	70	8.9
51124.8	3.62E-08	1.07E-07	1.37E-06	0.33816	0.980018	-18.46	53.65	74	9.9
51833.8	2.75E-08	4.14E-08	8.18E-07	0.664378	0.635575	13.16	74.37	64.4	2.9
52402.5	4.26E-08	6.41E-08	7.80E-07	0.664964	1.03262	17.99	69.03	69.4	5.6
52988.8	1.59E-07	2.20E-07	4.79E-06	0.722937	0.576672	0.00	47.33	76.2	3.7
53584.1	2.03E-07	3.06E-07	8.19E-06	0.66483	0.469031	-1.36	50.51	78.2	4.3
54170.5	7.73E-08	1.60E-07	2.63E-06	0.483591	0.762092	9.07	56.13	79.5	7.4
54742.1	1.53E-07	3.63E-07	6.29E-06	0.421753	0.726309	35.50	56.02	61.9	10.7
55322.5	1.52E-07	2.27E-07	5.05E-06	0.668087	0.56533	11.71	36.99	67.8	5.5
55908.5	1.54E-07	2.01E-07	6.96E-06	0.766462	0.361779	-13.45	31.26	64	5.5
56494.6	2.60E-07	4.25E-07	1.76E-05	0.6121	0.30387	-12.93	35.84	66.7	5.7
57099	4.21E-07	7.48E-07	3.20E-05	0.563701	0.293534	-11.50	52.44	77	7.6
57691.2	8.23E-07	2.43E-06	0.00012813	0.338623	0.238231	-2.55	57.84	81	5.4
58283.3	7.06E-07	1.98E-06	0.00012026	0.35683	0.206741	11.93	55.31	78.2	8.3
58878.6	3.56E-07	1.19E-06	5.83E-05	0.298329	0.257438	-9.26	65.56	75.4	4.8
59437.1	3.13E-07	1.24E-06	6.88E-05	0.252824	0.225952	12.31	33.21	65.4	5.3
60057	6.65E-07	2.36E-06	0.00013179	0.28189	0.225067	-16.21	45.98	71.2	7.9
60769	6.73E-07	1.02E-06	5.44E-05	0.65775	0.23625	34.71	58.18	63	10.5
61477.7	4.66E-07	1.20E-06	6.84E-05	0.388535	0.220435	24.26	41.07	64	9.1
62172.5	2.96E-07	6.18E-07	2.78E-05	0.478151	0.279665	0.44	38.51	70.7	2.9
62888.1	3.04E-07	7.64E-07	3.37E-05	0.398166	0.284751	-10.61	39.09	69.4	5.4
63596.7	3.51E-07	1.03E-06	4.18E-05	0.339652	0.311065	12.76	47.12	73.4	7
64284.7	1.64E-07	9.09E-07	3.12E-05	0.180789	0.366401	5.28	58.74	80.5	5.9

Table DR3. Incremental chronology

Depth (mm)	Age (yrs BP)	Growth rate (mm/kyr)	Depth (mm)	Age (yrs BP)	Growth rate (mm/kyr)
22.500	39192	4.24	29.168	40770	6.54
22.623	39221	4.24	29.522	40812	8.41
22.777	39266	3.41	29.772	40849	6.78
23.187	39392	3.25	29.859	40863	6.21
23.316	39434	3.07	30.312	40917	8.38
23.592	39551	2.37	30.410	40928	8.91
23.623	39564	2.37	30.724	40964	8.72
24.053	39742	2.42	30.860	41001	3.68
24.178	39763	5.95	30.952	41014	7.10
24.368	39813	3.80	31.149	41040	7.56
24.436	39833	3.37	31.423	41076	7.63
24.475	39847	2.80	31.448	41081	5.00
24.542	39870	2.91	31.669	41116	6.32
24.624	39894	3.40	31.771	41131	6.78
24.690	39909	4.43	32.016	41166	7.00
24.725	39917	4.41	32.282	41209	6.19
24.976	39977	4.18	32.368	41223	6.16
25.188	40017	5.29	32.578	41258	5.99
25.366	40048	5.76	32.648	41270	5.85
25.408	40057	4.67	32.740	41287	5.37
25.654	40109	4.73	32.922	41318	5.87
25.858	40156	4.34	33.086	41348	5.48
26.116	40214	4.44	33.460	41408	6.23
26.203	40229	5.82	33.767	41452	6.98
26.267	40242	4.96	33.963	41485	5.95
26.380	40261	5.91	34.192	41522	6.18
26.503	40281	6.18	34.359	41547	6.66
26.762	40331	5.18	34.610	41592	5.59
26.977	40373	5.11	34.688	41608	4.84
27.201	40417	5.09	34.760	41624	4.52
27.270	40432	4.62	34.793	41631	4.75
27.492	40466	6.51	34.898	41652	4.96
27.563	40482	4.45	34.977	41668	4.94
27.801	40523	5.80	35.281	41716	6.34
27.896	40552	3.29	35.503	41747	7.15
27.986	40569	5.26	35.607	41767	5.22
28.198	40611	5.05	36.266	41869	6.46
28.312	40630	6.00	36.410	41889	7.16
28.442	40646	8.16	36.478	41900	6.20
28.614	40677	5.52	36.573	41917	5.62
28.708	40694	5.54	37.191	42013	6.43
28.788	40708	5.70	37.623	42084	6.08
28.902	40728	5.71	37.766	42111	5.30
29.083	40757	6.26	38.100	42167	5.97

Fig. DR1. Confocal micrograph showing fluorescent annual layering in the studied speleothem.

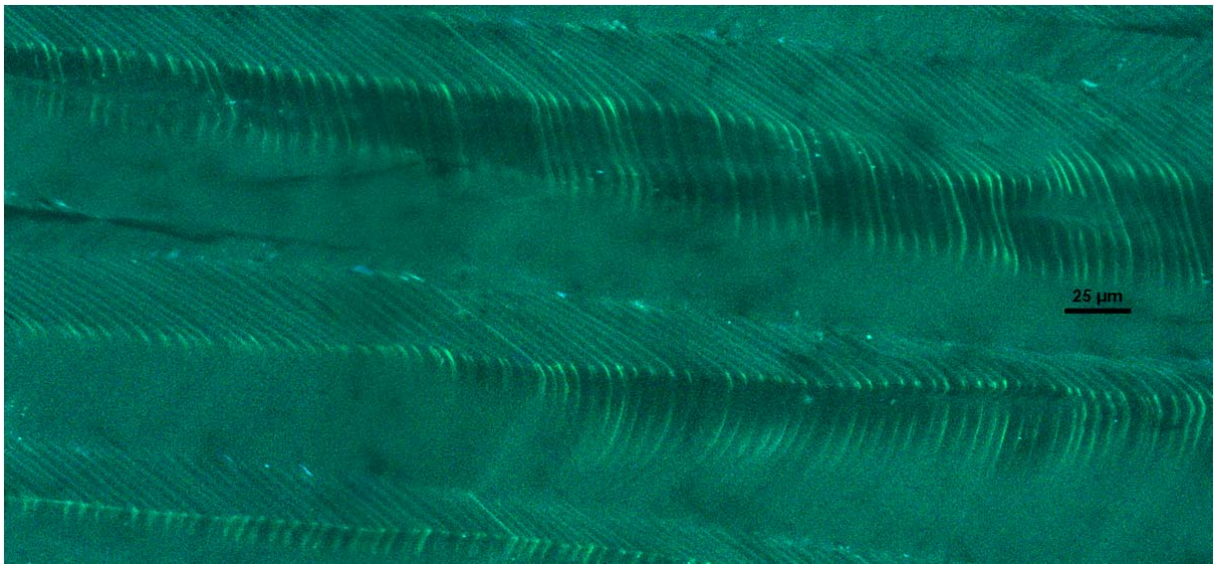

Fig. DR2. Orthogonal projection and azimuthal equidistant plot of the specimen from 62 ka BP. Full (open) squares represent the horizontal (vertical) projections of the demagnetization vectors (grey arrows). Magnetometer noise level is ~10^{-11} Am^2.